

Electron Spin Resonance Study of Monomeric, Dimeric, and Polymeric Acrylate Radicals Prepared Using the Atom Transfer Radical Polymerization Technique—Direct Detection of Penultimate-Unit Effects

Atsushi Kajiwara,^{*,†} Ajaya Kumar Nanda,[‡] and Krzysztof Matyjaszewski[‡]

Department of Materials Science, Nara University of Education, Takabatake-cho, Nara 630-8528, Japan, and Center for Macromolecular Engineering, Department of Chemistry, Carnegie Mellon University, 4400 Fifth Avenue, Pittsburgh, Pennsylvania 15213

Received October 8, 2003; Revised Manuscript Received November 26, 2003

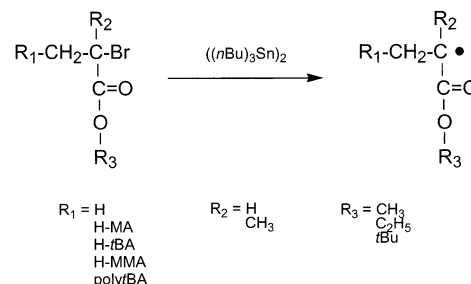
ABSTRACT: Model radicals generated through the reaction of organotin compounds with radical precursors prepared by atom transfer radical addition (ATRA) or atom transfer radical polymerization (ATRP) were studied by electron spin resonance (ESR). Dimers of various (meth)acrylate units, methyl acrylate (MA), *tert*-butyl acrylate (*t*BA), and methyl methacrylate (MMA), MA-MA-Br, MA-*t*BA-Br, *t*BA-*t*BA-Br, MMA-*t*BA-Br, and MA-MMA-Br, were prepared by ATRA. These dimers provided radicals mimicking the active species in a radical copolymerization of MA, MMA, and *t*BA. Well-resolved ESR spectra of the dimeric radicals confirm electronic and steric effects of the penultimate unit on the propagating radical. Hyperfine splitting constants observed for monomeric, dimeric, oligomeric, and polymeric *tert*-butyl acrylate radicals depend on the polymer chain length. The variation of ESR spectra with the chain length and penultimate unit was compared with the rate constants of activation in an ATRP using a CuBr/bpy catalyst system.

Introduction

The well-resolved spectra obtained from electron spin resonance (ESR) spectroscopy provide information not only on the structure, properties, and concentration of radicals but also on the initiating and propagating (oligomeric and polymeric) of radicals in radical polymerizations.^{1–5} Well-resolved ESR spectra in the radical polymerizations of styrene and its derivatives, diene compounds, methacrylates, and vinyl esters were studied in benzene or toluene solution under usual polymerization conditions.^{6–13} All of these spectra were reasonably well simulated as the corresponding propagating radicals. ESR spectra of primary propagating radicals were observed in a styrene polymerization initiated with an azo initiator (dimethyl 2,2'-azobisisobutyrate, MAIB) under irradiation¹² and have been observed in other systems.^{14,15} The values of the hyperfine splitting constants (hfc) of the radicals were slightly different from those determined for polymeric propagating radicals. The difference originated from a penultimate-unit effect from the initiating radical, which had a methyl methacrylate structure (H-MMA-) attached to one styrene unit. In another case, large amounts of midchain radicals in acrylate polymerizations were detected by ESR spectroscopy. The terminal propagating radicals had readily rearranged to form a midchain radical via a 1,5-hydrogen shift.¹³ Accordingly, ESR spectroscopy has given an unambiguous proof of several reactions involved in radical polymerization.

Atom transfer radical polymerization (ATRP) is one of the most widely applied polymerization techniques in the field of controlled/living radical polymerization. ATRP allows the preparation of a wide range of polymeric materials with controlled molecular weights and well-defined architectures.^{16–22} ESR was employed to

Scheme 1. Generation of Radicals from Corresponding Alkyl Bromides



examine the potential intermediates in ATRP and to provide a deeper understanding of the ATRP process, including identification of the structure and concentration of the paramagnetic species involved.^{12,13,23–32} The polymers formed in ATRP contain terminal carbon–halogen bonds, and Giese et al. (Scheme 1)³³ have reported that these bonds can be homolytically cleaved by reaction with organotin compounds. Accordingly, various radicals that model the end groups in an ATRP can be formed from the corresponding precursors prepared by atom transfer radical addition (ATRA) and ATRP, and the generated radicals can be studied by ESR spectroscopy. Variation of the chain length and composition of polymeric radical precursors elucidates the effect of chain length and penultimate units on the ESR spectra of the formed radicals. It was previously reported³⁴ that the ESR spectra of propagating *tert*-butyl methacrylate radicals show chain length dependency.

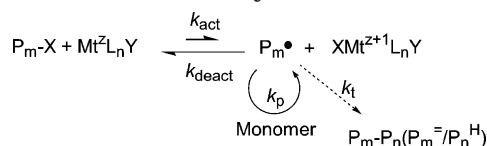
ATRP is based on a sequence of ATRA reactions, and accordingly, ATRA can be used to make various dimeric species modeling the expected chain ends in a copolymerization reaction. An ESR study of radicals generated from these mixed dimers can be used to clarify the penultimate-unit effects relevant to copolymerization. Direct ESR studies of penultimate-unit effects in real

* Corresponding author. E-mail: kajiwara@nara-edu.ac.jp.

[†] Nara University of Education.

[‡] Carnegie Mellon University.

Scheme 2. Elementary Reactions in ATRP



copolymerization reactions are extremely difficult due to the presence of many coexisting radical species. ESR spectra of monomeric radicals of (meth)acrylates were previously investigated by Fischer et al.,^{35–37} Gilbert et al.,^{38,39} and Matsumoto et al.^{40,41} However, no ESR study has so far been made for dimeric radicals of (meth)acrylates, mainly due to the difficulty of obtaining clean spectra in the experiments.

Recently, the rate constants of activation of monomeric and dimeric alkyl bromides with a CuBr/bpy complex as activator were determined. ATRP relies on the reversible activation of a dormant alkyl halide through halogen abstraction by a transition-metal complex to form a radical that participates in the classical free-radical polymerization scheme (Scheme 2) prior to deactivation. In this equilibrium, the alkyl radical (P_m^\bullet) is formed in an activation process, with a rate constant k_{act} , by the homolytic cleavage of an alkyl halogen bond ($\text{P}_m\text{-Z}$) catalyzed by a transition-metal complex in its lower oxidation state (Cu^{I}). The relative values of k_{act} of the alkyl bromides were determined for CuBr/bpy catalyst systems in acetonitrile at 35 °C, and they followed the order ethyl 2-bromoisobutyrate (EBriB) (30) \gg methyl 2-bromopropionate (MBrP) (3) $>$ *tert*-butyl 2-bromopropionate (*t*BBrP) (1) for monomeric initiators^{42,43} and MMA-MMA-Br (100) \gg MA-MMA-Br (20) $>$ MMA-MA-Br (5) $>$ MA-MA-Br (1) for dimeric initiators.⁴⁴

In this article, various dimeric acrylate and methacrylate model compounds were prepared by ATRA reactions as shown in Chart 1. Well-resolved ESR spectra were obtained, not only for the dimeric radicals but also monomeric and polymeric radicals, as shown in Chart 2. ESR was used to detect any chain length dependent spectroscopic changes for acrylate radicals and also the penultimate effect of different acrylate and methacrylate monomer units. The structure of the remote (penultimate) ester group does not affect ESR and that for the simplicity both ethyl methacrylate (EMA) and MMA were referred to as MMA.

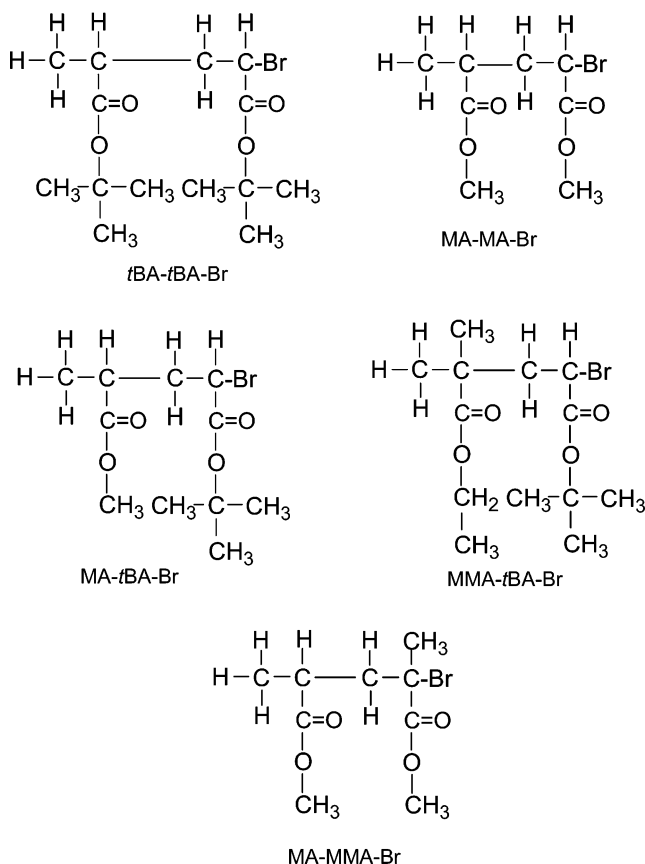
Experimental

Materials. $\text{Cu}^{\text{I}}\text{Br}$ (99%, Aldrich) was used after purification to remove any copper(II) species. EBriB (99%, Aldrich), ethyl 2-bromopropionate (EBrP) (99%, Aldrich), MBrP (99%, Aldrich), *tert*-butyl 2-bromopropionate (*t*BBrP) (99%, Aldrich), and *N,N,N',N'*-pentamethyldiethylenetriamine (PMDETA) (99%, Aldrich) were distilled under reduced pressure before use. *tert*-Butyl acrylate (*t*BA) was distilled over calcium hydride under reduced pressure and stored in the freezer before use. Dimethyl 2,2'-azobis(isobutyrate) (MAIB) (>97%, Wako), di-*tert*-butyl peroxide (*t*BPO) (>98%, Aldrich), and bis(tri-*n*-butyltin) ($(n\text{Bu})_3\text{Sn})_2$ (>90%, TCI) were used as received. All other reagents were purified before use.

Synthesis of Dimers. Dimers were synthesized via an atom-transfer radical-addition reaction using a molar excess of initiator compared to monomer, in the presence of a Cu^{I} /Cu^{II}PMDETA complex, to avoid polymerization.⁴⁴

All synthetic steps were carried out under nitrogen atmosphere. In a typical experiment, H-MA-MA-Br was synthesized as follows: $\text{Cu}^{\text{I}}\text{Br}$ (720 mg, 5×10^{-3} mol/L), $\text{Cu}^{\text{II}}\text{Br}_2$ (112 mg, 5×10^{-4} mol/L), and a magnetic stirring bar were introduced

Chart 1



into a predried round-bottom flask which was then tightly sealed with a rubber septum. Deoxygenated acetone (50 mL) followed by MA (430 mg, 5×10^{-3} mol/L) and PMDETA (956 mg, 5.5×10^{-3} mol/L) were introduced into the flask through a nitrogen-purged syringe and stirred until the system became homogeneous. Three "freeze-pump-thaw" cycles were performed to remove any oxygen from the reaction mixture. Finally, degassed MBrP (1.245 g, 7.5×10^{-3} mol/L) in 10 mL of acetone was introduced using a nitrogen-purged syringe and then the flask was placed in a thermostated oil bath at 35 °C. As soon as the initiator was added, the system turned dark green, indicating the progress of the reaction. After 2 h, the reaction was stopped by exposure to air and diluted with 20 mL of diethyl ether. The mixture was passed through an alumina column to remove the copper complex. The excess solvent was evaporated using a rotor evaporator. The excess MBrP was removed by vacuum. The dimer, H-MA-MA-Br, was collected by distilling the remaining mixture under a vacuum at ~ 1 Torr at 75 °C. H-MA-MA-Br was purified by two distillations, which gave 370 mg (25%) of the product. Purity was 99% by gas chromatography (GC). In GC, two signals were obtained associated to the presence of two diastereomers (i.e., a mixture of the racemic and meso forms of the dimer). ^1H NMR (600 MHz, CDCl_3): δ 4.37 (ddt, $J = 5.6, 4.8, 7.5$ Hz, 1H, CHBr), 3.80 (ss, 3H, $(\text{CH}-\text{Br})\text{COOCH}_3$), 3.71 (ss, 3H, $(\text{CH})\text{COOCH}_3$), 2.65–2.38 (m, 1H, CH), 2.20–2.03 (m, 2H, CH_2), 1.26 (dd, $J = 7.8, 7.2$ Hz, 3H, CH_3).

Similarly, H-MA-*t*BA-Br was synthesized using MBrP as the initiator in the presence of *t*BA. Purity was 99% by GC. In GC, two signals with nearly similar retention times were obtained for the two diastereomers. ^1H NMR (600 MHz, CDCl_3): δ 4.24 (ddt, $J = 4.9, 4.9, 8.1$ Hz, 1H, CHBr), 3.71 (ss, 3H, COOCH_3), 2.64–2.32 (m, 1H, CH), 2.16–1.98 (m, 2H, CH_2), 1.49 (ss, 9H, $\text{COOC}(\text{CH}_3)_3$), 1.25 (dd, $J = 7.0, 7.0$ Hz, 3H, CH_3).

H-*t*BA-*t*BA-Br was synthesized using *t*BBrP as the initiator in the presence of *t*BA. Purity was 99% by GC. In GC, two

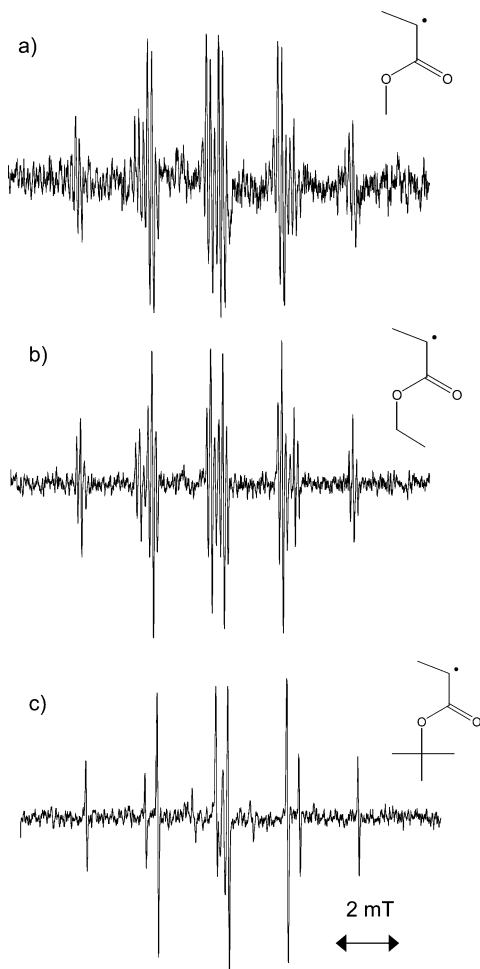


Figure 1. ESR spectra of generated radicals from corresponding alkyl bromides observed at 30 °C: (a) H-MA•; (b) H-EA•; and (c) H-*t*BA•.

lamp (Ushio USH-500D) at a distance of ca. 15 cm from the tube in the cavity. An IR-cut filter (Toshiba IRA-25S) was used.

Polymeric Model Radicals. P_tBA ($P_n = 15$) (50 mg, ca. 2.5×10^{-5} mol), $((n\text{Bu})_3\text{Sn})_2$ (4.5 mg, 2.5×10^{-5} mol), and *t*BPO (3.7 mg, 2.5×10^{-5} mol) were dissolved in toluene (150 mg) in a quartz tube (o.d. 5.0 mm). The solution was flushed with dry argon for several minutes and was placed in an ESR cavity. Radicals were generated under UV irradiation at −30 °C.

ESR Detection of Propagating Radicals of *t*BA in situ. *t*BA (30 mg, 2.3×10^{-4} mol) and *t*BPO (2.0 mg, 1.4×10^{-5} mol) were dissolved in toluene (170 mg) in a quartz tube (o.d. 5 mm). The solution was irradiated with UV light in an ESR cavity to initiate polymerizations at −30 °C. Formed propagating radicals were observed by ESR. ESR spectra of propagating radicals of MMA were also observed in a similar manner at 0, 30, 60, and 90 °C.

ESR Spectroscopy. The ESR spectra of the radicals were recorded on a JEOL JES RE-2X spectrometer operating in the X-band, utilizing a 100-kHz field modulation and a microwave power of 1 mW. A TE₀₁₁ mode cavity was used. Temperature was controlled by a JEOL DVT2 variable-temperature accessory. ESR measurements were performed at 90, 60, 30, 0, −15, and −30 °C in toluene. Spectroscopic simulations were carried out by a JEOL IPRIT Data Analysis System.

Molecular weights and molecular weight distributions were roughly estimated using a TOSOH CCP&8020 series GPC system with TSK gel columns. Polystyrene standards were used to calibrate the columns.

Activation Rate Constants Measurements. The activation rate constants for the various monomeric and dimeric

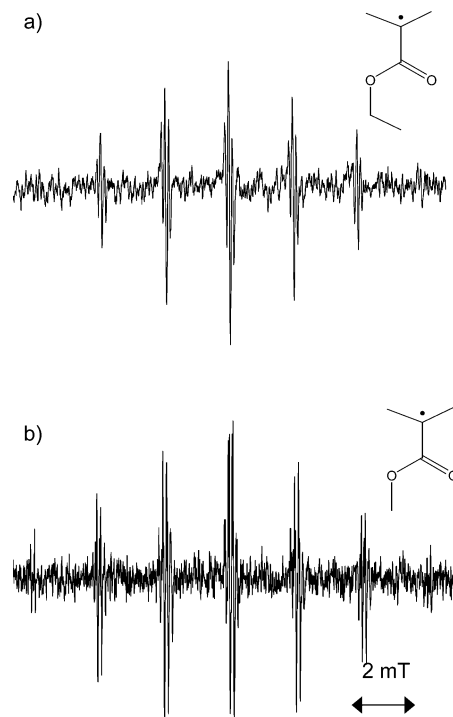


Figure 2. ESR spectra of monomeric methacrylate model radicals observed at 30 °C: (a) H-EMA• and (b) H-MMA•.

bromides were determined by the method described in the previous paper.⁴³

Results

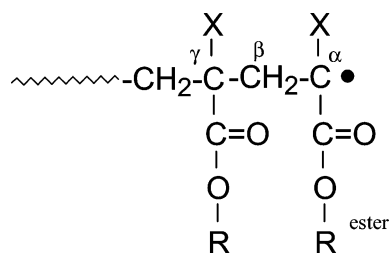
Observation of ESR Spectra. Monomeric Model Radicals. Radicals were generated by three methods: homolytic cleavage of carbon–bromine bonds of the alkyl bromides with hexabutyldistannane, photodecomposition of an azo initiator, and radical polymerization performed directly in a sample cell.

The ESR spectra of the radicals generated from monomeric alkyl bromides were studied first. MBrP, EBrP, and *t*BBrP provided radicals that model monomeric methyl acrylate (H-MA•), ethyl acrylate (H-EA•), and *tert*-butyl acrylate (H-*t*BA•), respectively, by reactions with organotin compounds. As shown in Figure 1, clear and well-resolved spectra were observed. Values of hfc were precisely determined from the spectra, and these spectra were reasonably simulated with the obtained hfc values. The values of hfc from these radicals and the other model radicals are summarized in Table 1. Two sets of quartets were observed in each spectrum, indicating a presence of three equivalent protons and one more proton with a different coupling constant.

In the cases of H-MA• and H-EA•, each spectroscopic line has an additional splitting in the form of a fine quartet (0.145 mT) and triplet (0.138 mT), respectively, due to methyl and methylene protons in the ester side groups. It means that the spin density is delocalized through the ester bonds. In the case of H-*t*BA•, splitting due to methyl groups in the *tert*-butyl group is too small to be observed. They are included in the line width. These findings indicate the formation of radicals with the expected structures, as shown in Chart 1.

The hydrogenated monomeric model radical of ethyl methacrylate (H-EMA•) was formed in the reaction of EBriB with organotin compounds. A clear and well-resolved ESR spectrum was observed (Figure 2a), and

Table 1. Hyperfine Splitting Constants of Radicals Measured at 30 °C



radicals	source	hfc, mT				line width ^a
		α	β	γ	ester	
H-MA•	MBrP	2.130	2.555		0.145	0.051
H-EA•	EBrP	2.134	2.547		0.138	0.040
H- <i>t</i> BA•	<i>t</i> BBrP	2.090	2.550			0.040
H-EMA•	EBriB		2.220		0.128	0.047
H-MMA•	MAIB		2.225		0.128	0.039
H-MA- <i>t</i> BA•	MA- <i>t</i> BA-Br	2.070	2.270	0.078		0.040
H- <i>t</i> BA- <i>t</i> BA•	<i>t</i> BA- <i>t</i> BA-Br	2.090	2.270	0.078		0.047
H-MA-MA•	MA-MA-Br	2.07	2.29	0.08	0.1	0.039
H-MA-MMA• ^b	MA-MMA-Br		2.260 (CH ₃)	0.080	0.128	0.055
			1.480 (CH ₂)			
H-MMA- <i>t</i> BA•	MMA- <i>t</i> BA-Br	2.090	2.210			0.047
poly <i>t</i> BA• ^c	poly <i>t</i> BA-Br	2.28	2.06			0.12
polyMMA• ^b	MMA (in situ)		2.22 (CH ₃)		0.11	0.050
			1.44 (β-CH)			
			0.97 (β-CH)			

^a Line width at half height. ^b Measured at 90 °C. ^c Measured at −30 °C.

interpretation of the spectrum confirms the formation of a radical with the structure shown in Chart 1. The hydrogenated monomeric methyl methacrylate (H-MMA•) radical was generated through photodecomposition of MAIB under irradiation. The ESR spectra of monomeric methacrylate radicals are shown in Figure 2b. The values of hfc are summarized in Table 1.

ESR spectra of H-EA•, H-EMA•, and H-MMA• were reported previously and the values of hfc in that study are comparable to the results obtained in the present study.^{40,47}

Dimeric Model Radicals. The dimeric model compounds studied can be classified into two groups. The terminal radical can have either an acrylate or a methacrylate structure. Dimeric model radicals with an acrylate terminal group were generated in the reaction of the corresponding alkyl bromides (*t*BA-*t*BA-Br, MA-*t*BA-Br, MMA-*t*BA-Br, and MA-MA-Br) with an organotin compound under irradiation. The resulting radicals had structures of hydrogenated dimeric radicals, i.e., H-*t*BA-*t*BA•, H-MA-*t*BA•, H-MMA-*t*BA•, and H-MA-MA•, respectively. Observed ESR spectra of these radicals are presented in Figure 3. As shown in the figure, clear and well-resolved spectra were observed and precise values for hfc can be determined from the spectra. The hfc values are included in Table 1. A doublet of triplets was observed in each spectrum and can be assigned to the α proton and two equivalent β-methylene protons, respectively.

The model dimeric H-MA-MMA• radicals were generated by reacting the corresponding alkyl bromide (MA-MMA-Br) with an organotin compound under irradiation. ESR spectra were performed at 30, 60, and 90 °C. The spectrum of H-MA-MMA• at 90 °C, along with its simulation, is shown in Figure 4. A 12-line spectrum with a very small quartet in each spectroscopic line was detected. The 12-line spectrum is caused by a quartet of triplets (4 × 3) from three equivalent methyl protons

and two methylene protons. An additional very small splitting of a doublet (0.080 mT) due to the γ proton in the MA moiety can also be observed. The signal intensity of each spectroscopic line displays a temperature-dependent change due to hindered rotation around the C_α–C_β bond.^{3,12,34} At 90 °C, the bond rotates freely and the spectrum was simulated as shown in Figure 4.

ESR spectra of such model dimeric radicals with well-defined structures have not been observed before. Analyses of the values obtained from the hfc clearly show the dimeric radicals have the structures indicated in Chart 1.

Polymeric Radicals. The ESR spectrum of the propagating radical for *t*BA polymerization was measured in situ at −30 °C. The reaction was conducted at −30 °C since, at temperatures higher than −30 °C, a 1,5-hydrogen shift chain-transfer reaction occurs forming a large amount of midchain radicals. ESR spectra of propagating radicals were obtained at −30 °C, although the line width of the spectra is greater than those seen in monomeric and dimeric model radicals. A doublet of triplets, which should be due to an α proton and β-methylene protons, can be observed in the spectra allowing the precise determination of the hfc values. The splitting from the γ proton, which was observed in the spectra of dimers, disappeared within the line width. Oligomeric model radicals, with 15 monomer units of *t*BA (DP_n = 15), were also generated from corresponding oligomeric alkyl bromide prepared by ATRP. The radicals were also studied by ESR at −30 °C.

Radical polymerization of MMA initiated with di-*tert*-butyl peroxide (*t*BPO) was performed in an ESR sample cell in the cavity under irradiation at 90 °C. An ESR spectrum of the propagating radicals of MMA was recorded. A clear and well-resolved spectrum was obtained. Values of hfc for these polymeric radicals are summarized in Table 1.

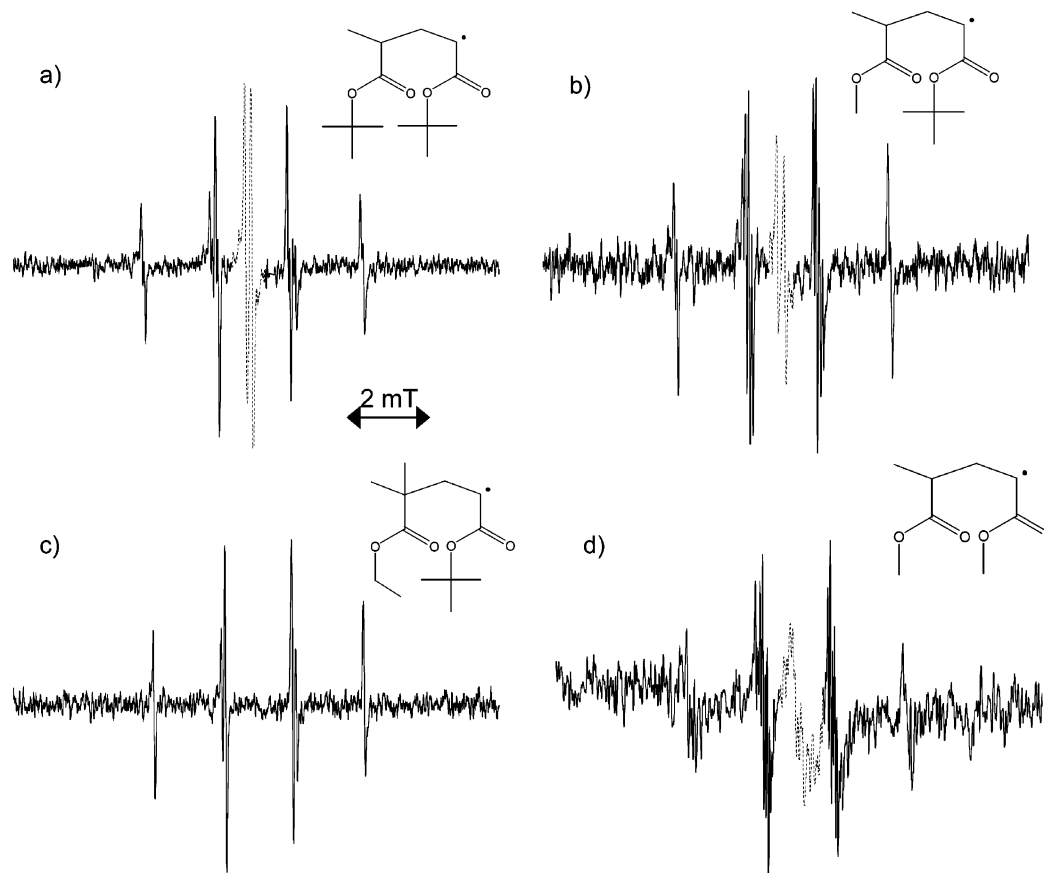


Figure 3. ESR spectra of dimeric model radicals generated from corresponding alkyl bromides observed at 30 °C: (a) H-*t*BA-*t*BA•; (b) H-MA-*t*BA•; (c) H-MMA-*t*BA•; and (d) H-MA-MA•. Spectroscopic lines appearing at the center of the spectra (indicated by dashed line) are due to radicals of tin compounds.

Discussion

Dimeric Radicals and Penultimate-Unit Effect.

Penultimate-unit effects were observed in the ESR spectra of model dimeric radicals. The ESR spectra of dimeric radicals with acrylate terminal units will be discussed first. When we compare the spectrum of H-MMA-*t*BA• with that of H-MA-*t*BA• or H-*t*BA-*t*BA•, we can see the effect of a methacrylate penultimate unit (this is the effect of the presence of a methyl group at the γ position). The presence of an MMA unit shows only small variations in the couplings of the α proton. Obviously, the spin density at the α carbon atom does not change appreciably by β substitution. On the other hand, the couplings of β -methylene protons vary considerably with the presence of an MMA penultimate unit as shown in Table 1. The value of hfc at β -methylene protons for H-MMA-*t*BA• (2.210 mT) is smaller than that of H-MA-*t*BA• (2.270 mT) or of H-*t*BA-*t*BA• (2.270 mT). ESR spectra of monomeric acrylic acid radicals with various substituents, i.e., HO-, NH₂-, CH₃-, HO-CH₂-, were previously discussed by Fischer et al.,³⁵ and the reported values of hfc 's of the β protons varied considerably with the substituents. Judging from the reported results, the electronic effect of a penultimate MMA unit is larger than those of substituents. These findings show an electron-withdrawing effect of the MMA unit. Steric effect of the presence of the γ methyl group may have appeared in the broader line width than that in the case of H-MA-*t*BA•. In comparison with ESR spectrum of H-MA-*t*BA•, the steric effect of H-*t*BA-*t*BA• appeared in the line width of the spectrum, although the electronic effect of replacement of a

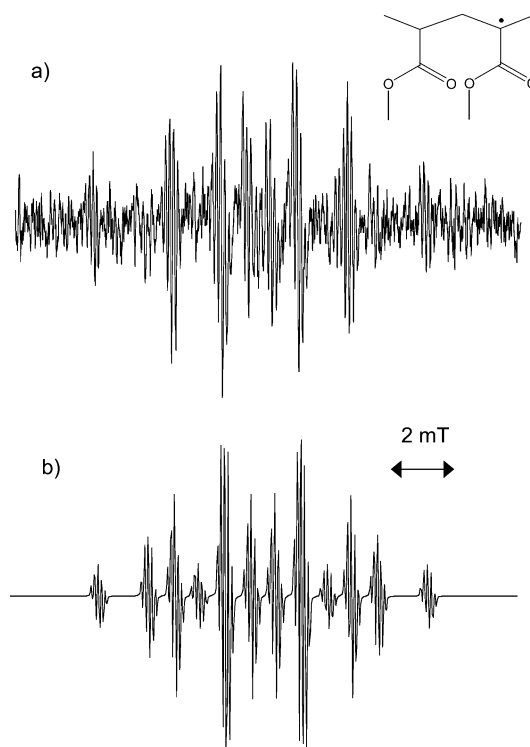


Figure 4. Observed (a) and simulated (b) ESR spectra of H-MA-MMA• observed at 90 °C.

methyl group by a *tert*-butyl group is very small. Sterically, the small ester methyl group of MA caused less hindrance to the rotation of the C $_{\beta}$ -C $_{\alpha}$ bond. As a

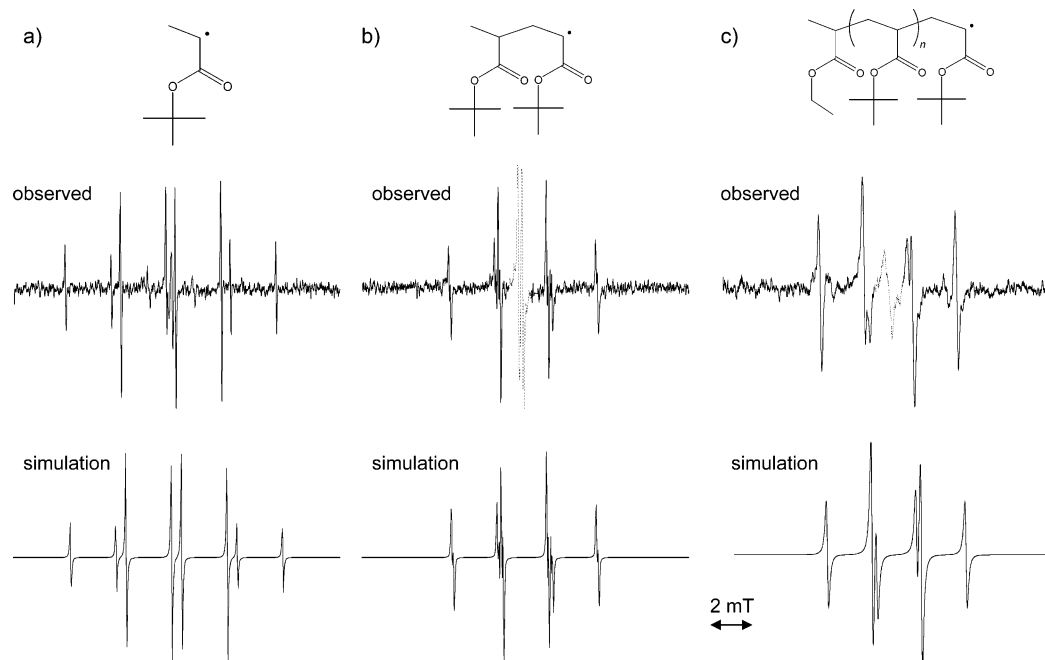


Figure 5. Observed and simulated ESR spectra of *t*BA radicals with various chain lengths observed at 30 °C: (a) H-*t*BA• (monomeric); (b) H-*t*BA-*t*BA• (dimeric); and (c) H-(*t*BA)_{*n*}-*t*BA• (polymeric model radicals, *n* ~ 15 (DP_{*n*} = 15)). Spectroscopic lines appearing at the center of the spectra (indicated by dashed line) are due to radicals of tin compounds.

Table 2. Hyperfine Splitting Constants of *t*BA Radicals with Various Chain Lengths

radicals	source	hfc (mT)			reference
		α	β	γ	
H- <i>t</i> BA•	<i>t</i> BrP	2.090	2.550		this work
H- <i>t</i> BA- <i>t</i> BA•	<i>t</i> BA- <i>t</i> BA-Br	2.090	2.270	0.078	this work
H-(<i>t</i> BA) _{<i>n</i>} •	(<i>t</i> BA) _{<i>n</i>} -Br	2.28	2.06		56
poly A (poly(acrylic acid))	acrylic acid (in situ)	2.067	2.206		37
poly B (poly(acrylic acid))	acrylic acid (in situ)	2.262	2.134		37

result, a clear separation of spectroscopic lines, due to narrower line width, was observed. This difference in ESR spectra between H-MMA-*t*BA• and H-*t*BA-*t*BA• suggests that the reactivity of the terminal *t*BA radical may depend on the penultimate unit in copolymerizations of MMA and *t*BA.

Radical copolymerization of MA (M₁) and MMA (M₂) was investigated and *r*₁ and *r*₂, copolymer reactivity ratios, were determined to be 0.4 and 2.15, respectively.⁴⁸ However, these results were obtained without considering the penultimate-unit effect. The present ESR results for H-MA-MMA•, H-MA-MA•, and H-MMA-*t*BA• suggest the presence of penultimate-unit effects on the acrylate terminal unit.

Thus, electronic and steric penultimate effects influence not only radical reactivity^{49–55} but also their ESR spectra.

Polymeric Radicals and Chain Length Dependent Change in ESR Spectra. The ESR spectra of H-*t*BA•, H-*t*BA-*t*BA•, and poly(*t*BA)• (DP_{*n*} = 15), where the radicals were generated from the corresponding alkyl bromides, are shown in Figure 5 along with their simulations.

In the monomeric and dimeric radicals, the coupling constants for the α proton are smaller than those for the β protons. However, in the case of polymeric radicals, with DP_{*n*} = 15, the coupling constant for the α proton was larger than those for the β protons as shown in Figure 5c and Table 2. The ESR spectra of *t*BA polymeric radicals with DP_{*n*} = 50, DP_{*n*} = 100, and propagating radicals in situ were very similar to that

of DP_{*n*} = 15.^{13,56} This can indicate either a penultimate-unit effect or another chain-length effect. Therefore the origin of the chain length dependent variation of the ESR spectra is not yet explained.

Fischer et al. reported ESR spectra of polymeric radicals of acrylic acid by a flow method and detected two kinds of radical species with different coupling constants. They named them as polymeric radicals A and B, respectively. The coupling constants for α and β protons were reported to be 2.067 and 2.206 mT for A and 2.262 and 2.134 mT for B. In the case of radical A, although they were different from those of monomeric radicals, the coupling constant for the α proton was smaller than that for β protons. In the case of radicals B, the value of the hfc for the α proton was larger than that seen for β -methylene protons. A similar dependence was found for *t*BA-derived radicals in this work. These results could indicate that radical A was an oligomeric radical (longer than dimeric) and that radical B had a longer chain length than radical A.

Chain length dependent ESR spectra were also observed for methacrylate radicals. Apparently, the coupling constant of two β -methylene protons changed from equivalent to nonequivalent as the chain length increased. However, coupling constants of protons in methyl group at α position do not show any chain length dependent change. The exchange of the magnitude of hfc values between α and β protons in acrylates is therefore solely characteristic to the acrylates. Chain length dependent spectroscopic change in

methacrylates will be discussed in detail in the following article.⁵⁷

Activation Rate Constants for Monomeric and Dimeric Alkyl Bromides and ESR Spectra. The relative values of k_{act} for alkyl bromides follow the order EBriB (30) \gg MBrP (3) $>$ tBrP (1). This order not only indicates higher thermodynamic stability of the tertiary radicals (H-EMA \cdot) but also lower reactivity of the secondary radical with a bulkier *tert*-butyl group rather than the smaller methyl group. This was explained by suggesting steric hindrance in the atom-transfer process where the catalyst complex must approach the halogen atom. However, judging from the values of h_{fc} for H-tBA \cdot , H-MA \cdot , and H-EA \cdot , electronic effect from the ester side groups seems negligibly small. Thus, replacement of a methyl group (MBrP) by a *tert*-butyl group (tBrP) has no significant effect on the values of the h_{fc} determined in the ESR spectra, but the steric effect in the transition state for atom transfer leads to a 3-fold difference in k_{act} .

The values of k_{act} for the dimeric bromides follow the order MMA-MMA-Br (100), MA-MMA-Br (20), MMA-MA-Br (5), and MA-MA-Br (1). Differences between MMA-MMA-Br and MA-MMA-Br, and between MMA-MA-Br and MA-MA-Br, may be explained similarly to MA-tBA and MMA-tBA systems. When a MMA unit is located in the penultimate position, values of h_{fcs} of β protons of tBA were smaller than with MA as the penultimate unit. These electronic effect and steric effects manifest themselves in different values of k_{act} .

We anticipate that a combination of ESR analysis and kinetic studies will lead to a better understanding of both the structure and the reactivity of the radicals. Such information is very important for basic research, not only for ATRP but also for conventional radical polymerization processes.

Acknowledgment. This research was supported in part by a Grant-in-Aid (No. 15550107) from the Ministry of Education, Culture, Sports, Science, and Technology of Japan. Financial support from the National Science Foundation (CHE-0096601) is gratefully acknowledged.

References and Notes

- Fischer, H. *Adv. Polym. Sci.* **1968**, *5*, 463.
- Fischer, H. In *Polymer Spectroscopy*; Hummel, D. O., Ed.; Springer-Verlag: Weinheim, Germany, 1974; pp 289–354.
- Kamachi, M. *Adv. Polym. Sci.* **1987**, *82*, 207.
- Yamada, B.; Westmoreland, D. G.; Kobatake, S.; Konosu, O. *Prog. Polym. Sci.* **1999**, *24*, 565.
- Kamachi, M. *J. Polym. Sci., Part A: Polym. Chem.* **2002**, *40*, 269.
- Kamachi, M.; Kajiwar, A. *Macromol. Symp.* **2002**, *179*, 53.
- Kamachi, M.; Kajiwar, A. *Macromolecules* **1996**, *29*, 2378.
- Kamachi, M.; Kajiwar, A. *Macromol. Chem. Phys.* **1997**, *198*, 787.
- Kamachi, M.; Kajiwar, A. *Macromol. Chem. Phys.* **2000**, *201*, 2165.
- Kajiwar, A.; Kamachi, M. *Macromol. Chem. Phys.* **2000**, *201*, 2160.
- Kamachi, M. In *Controlled Radical Polymerization*; Matyjaszewski, K., Ed.; ACS Symposium Series 685; American Chemical Society: Washington, DC, 1998; Chapter 9, pp 145–168.
- Kajiwar, A.; Matyjaszewski, K.; Kamachi, M. In *Controlled/Living Radical Polymerization*; Matyjaszewski, K., Ed.; ACS Symposium Series 768; American Chemical Society, Washington, DC, 2000; Chapter 5, pp 68–81.
- Kajiwar, A.; Kamachi, M. In *Advances in Controlled/Living Radical Polymerization*; Matyjaszewski, K., Ed.; ACS Symposium Series 854; American Chemical Society, Washington, DC, 2003; Chapter 7, pp 86–100.
- Tanaka, H.; Sasai, K.; Sato, T. *Macromolecules* **1988**, *21*, 3534.
- Sato, T.; Inui, S.; Tanaka, H.; Ota, T.; Kamachi, M.; Tanaka, K. *J. Polym. Sci., Part A: Polym. Chem.* **1987**, *25*, 637.
- Wang, J.-S.; Matyjaszewski, K. *J. Am. Chem. Soc.* **1995**, *117*, 5614.
- Wang, J.-S.; Matyjaszewski, K. *Macromolecules* **1995**, *28*, 7901.
- Patten, T. E.; Matyjaszewski, K. *Adv. Mater.* **1998**, *10*, 901.
- Coessens, V.; Pintauer, T.; Matyjaszewski, K. *Prog. Polym. Sci.* **2001**, *26*, 337.
- Matyjaszewski, K.; Xia, J. *Chem. Rev.* **2001**, *101*, 2921.
- Kamigaito, M.; Ando, T.; Sawamoto, M. *Chem. Rev.* **2001**, *101*, 3689.
- Davis, K. A.; Matyjaszewski, K. *Adv. Polym. Sci.* **2002**, *159*, 2.
- Knuehl, B.; Pintauer, T.; Kajiwar, A.; Fischer, H.; Matyjaszewski, K. *Macromolecules* **2003**, *36*, 8291.
- Zhou, W.; Zhu, S. *Ind. Eng. Chem. Res.* **1997**, *36*(4), 1130.
- Matyjaszewski, K.; Kajiwar, A. *Macromolecules* **1998**, *31*, 548.
- Kajiwar, A.; Matyjaszewski, K. *Macromol. Rapid Commun.* **1998**, *19*, 319.
- Kajiwar, A.; Matyjaszewski, K.; Kamachi, M. *Macromolecules* **1998**, *31*, 5695.
- Kajiwar, A.; Matyjaszewski, K. *Polym. J.* **1999**, *31*, 70.
- Yu, Q.; Zeng, F.; Zhu, S. *Macromolecules* **2001**, *34*, 1612.
- Wang, A. R.; Zhu, S. *Polym. Prepr. (Am. Chem. Soc., Div. Polym. Chem.)* **2002**, *43*(2), 11.
- Wang, A. R.; Zhu, S. *Macromolecules* **2002**, *35*, 9926.
- Wang, A. R.; Zhu, S.; Matyjaszewski, K. In *Advances in Controlled/Living Radical Polymerization*; Matyjaszewski, K., Ed.; ACS Symposium Series 854; American Chemical Society, Washington, DC, 2003; Chapter 12, pp 161–179.
- Giese, B.; Damm, W.; Wetterich, F.; Zeitz, H.-G. *Tetrahedron Lett.* **1992**, *33*, 1863.
- Kajiwar, A.; Maeda, K.; Kubo, N.; Kamachi, M. *Macromolecules* **2003**, *36*, 526.
- Fischer, H.; Giacometti, G. *J. Polym. Sci. C* **1967**, *16*, 2763.
- Fischer, H. *Z. Naturforsch.* **1964**, *19a*, 267.
- Fischer, H. *Z. Naturforsch.* **1964**, *19a*, 866.
- Gilbert, B. C.; Lindzay Smith, J. R.; Milne, E. C.; Whitwood, A. C.; Taylor, P. *J. Chem. Soc., Perkin Trans. 2* **1993**, 2025.
- Gilbert, B. C.; Lindzay Smith, J. R.; Milne, E. C.; Whitwood, A. C.; Taylor, P. *J. Chem. Soc., Perkin Trans. 2* **1994**, 1759.
- Matsumoto, A.; Giese, B. *Macromolecules* **1996**, *29*, 3758.
- Spichty, M.; Giese, B.; Matsumoto, A.; Fischer, H.; Gescheidt, G. *Macromolecules* **2001**, *34*, 723.
- Nanda, A. K.; Matyjaszewski, K. *Macromolecules* **2003**, *36*, 599.
- Nanda, A. K.; Matyjaszewski, K. *Macromolecules* **2003**, *36*, 1487.
- Nanda, A. K.; Matyjaszewski, K. *Macromolecules* **2003**, *36*, 8222.
- Ando, T.; Kamigaito, M.; Sawamoto, M. *Tetrahedron* **1997**, *53*, 15445.
- Davis, K. A.; Matyjaszewski, K. *Macromolecules* **2000**, *33*, 4039.
- Tanaka, H.; Kagawa, T.; Sato, T. *Macromolecules* **1986**, *19*, 934.
- Zubov, V. P.; Valuev, L. I.; Kabanov, V. A.; Kargin, V. A.; *J. Polym. Sci. A-1* **1971**, *9*, 833.
- Giese, B.; Engelbrecht, R. *Polym. Bull.* **1984**, *12*, 55.
- Fukuda, T.; Ma, Y.-D.; Inagaki, H. *Makromol. Chem., Suppl.* **1985**, *12*, 125.
- Fukuda, T.; Ma, Y.-D.; Inagaki, H. *Macromolecules* **1985**, *18*, 17.
- Ma, Y.-D.; Fukuda, T.; Inagaki, H. *Macromolecules* **1985**, *18*, 26.
- Cywar, D. A.; Tirrell, D. A. *Macromolecules* **1986**, *19*, 2908.
- Prementine, G. S.; Tirrell, D. A. *Macromolecules* **1987**, *20*, 3034.
- O'Driscoll, K. F.; Davis, T. P. *J. Polym. Sci., C* **1989**, *27*, 417.
- Kajiwar, A.; Amano, N.; Kamachi, M. To be published.
- Kajiwar, A.; Kamachi, M. To be published.